UNIVERSITY OF LEEDS

This is a repository copy of *Straight leg walking strategy for torque-controlled humanoid robots*.

White Rose Research Online URL for this paper:
http://eprints.whiterose.ac.uk/144476/

Version: Accepted Version

eprints@whiterose.ac.uk
https://eprints.whiterose.ac.uk/

Straight Leg Walking Strategy for Torque-controlled Humanoid Robots

Yangwei You, Songyan Xin, Chengxu Zhou, Nikos Tsagarakis

Abstract— Most humanoid robots walk in an unhuman-like way with bent knees due to the use of the simplified Linear Inverted Pendulum Model (LIPM) which constrains the Center of Mass (CoM) in a horizontal plane. Therefore it results in high knee joint torque and extra energy consumption. To address this issue, we propose a simple yet efficient control strategy to realize straight leg walking. First, theoretical analyses of simplified models provide insight into Zero Moment Point (ZMP) deviations during straight knee walking. Based on the finding that the deviation is limited comparing to the support polygon, we decide to keep using the LIPM for high-level planning, but let the robot perform straight leg walking automatically via the optimization-based low-level controller. By setting the desired CoM height slightly over the robot's reachable height, the low-level controller will attempt to straighten the robot's leg to reach this vertical reference, in the meanwhile, also satisfy the constraints (i.e. dynamic feasibility, friction cone, torque limits). The simulation results of the humanoid robot WALK-MAN demonstrate the feasibility of proposed control strategy with relatively high energy efficiency. A typical butterfly shape of CoM trajectory was also observed in the frontal plane which is common in human walking.

I. INTRODUCTION

Human walks in a pendulum-like manner to make their muscles work efficiently [1]. This pendular mechanism is the consequence of the straightened leg during walking, which makes it easier for the leg muscles to accelerate the Center of Mass (CoM) and support body weight, therefore improving the energy efficiency [2]. But how to make the bipedal robots walk in such a energy efficient way? One of the best examples is the passive dynamic walker which could perform human-like gait with no actuations but only gravity [3]. The passive dynamic walker has demonstrated several human walking characteristics such as stretched-knees, heel-strike and toe-off. However, these motions are rarely seen on their powered companions, the actuated humanoids, despite most of them have very similar physical capabilities comparing to human. There exists no particular reason why these robots could not perform energy efficient walking with straightened leg as human does. A main practical reason lies in the control strategy used to generate walking motions.

Simplified models are often used to abstract the whole body dynamic of humanoid robot. Linear Inverted Pendulum Model (LIPM) [4] approximates the whole robot as a point mass which is constrained in a predefined plane. The point mass was later replaced by a flywheel to introduce angular momentum about the CoM, and this leads to the Linear
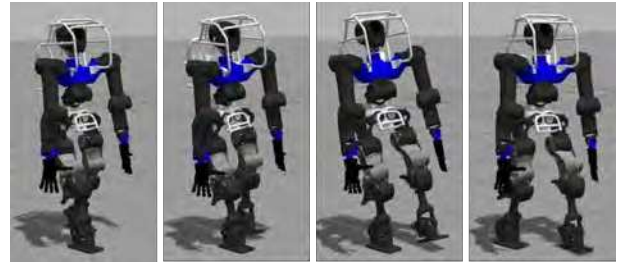
Fig. 1. Snapshots of WALK-MAN straight leg walking (time interval 0.5s).

Inverted Pendulum Plus Flywheel Model [5]. These two models are usually used to generate walking pattern for humanoid robots. However, the robots need to walk with bent knees due to the assumption of constant CoM height. Adding two massless spring legs to the point mass produces the Spring Loaded Inverted Pendulum (SLIP) [6] which is better when considering the compliant behaviors observed in human walking. Although the motion generated by SLIP model is more natural than LIPM, its nonlinear characteristic makes it difficult for on-line planning.

Many studies have taken CoM height variation into consideration for planning in order to generate more human-like walking motion. Howerver, introducing CoM vertical motion leads to the nonlinear Zero Moment Point (ZMP) constraints. Different approaches have been proposed to address the nonlinearity. One way is to define the vertical motion beforehand, then the ZMP constraints will be still linear and could be solved via linear approaches. Limiting CoM to a sculptured surface, CoM trajectory can be uniquely defined along the surface satisfying the ZMP constraint [7]. Given CoM vertical oscillation, analytic solution is proposed to cooperate the vertical motion with horizontal ones [8]. Li *et al.* [9] proposed virtual spring-damper model to generate the vertical CoM motion which is independent from the horizontal motions. Englsberger *et al.* realized 3D walking based on the divergent component of motion [10]. Particularly, the humanoid WABIAN [11] could perform knee stretching walking by predefining the trajectory of support-leg's knee joint, and it could also realize heel-contact and toe-off motions with specially designed passive toe joints. Inspired by Raibert's work [12], [13] realized humanoid-like walking by determining foot placement via on-line linear regression, however it is hard to fully utilize ankle torque to help stabilizing.

Considering the nonlinear ZMP constraint, a way to generate 3D CoM motion is presented in [14] in which the

ZMP constraint is expressed in quadratic form and then the problem can be solved as a quadratically constrained quadratic program. In order to handle the height variations on rough terrain, Feng *et al.* [15] generated 3D CoM trajectory using Differential Dynamic Programming with explicitly added vertical component to their CoM model. These nonlinear numerical techniques are usually computer-intensive. Approaches transferring nonlinearity into linearity by approximating the nonlinear bounds with linear ones have been proposed in [16], the 3D CoM motion generation problem can be included directly into a LMPC scheme with those new bounds.

The above mentioned methods either need specific design of the vertical CoM motion, or demand heavy computational power. Therefore, in this paper, we introduce a simple yet efficient strategy to realize straight leg walking on a torque-controlled humanoid robot. Starting with the analyses of the ZMP deviation caused by the CoM vertical motion, we find out this deviation is not critical comparing to the stability margin of ZMP. Therefore, we propose to release the tracking of CoM vertical motion in low level controller, nevertheless the deviated ZMP will still be constrained inside support polygon through proper distribution of GRF by the low-level controller.

This paper is organized as follows. In Section II, a model is applied to analyze the ZMP behavior caused by the CoM vertical motion and demonstrate the feasibility of proposed strategy. Section III presents the overall control framework including a high-level controller in which CoM trajectory and foot placement are generated and a low-level controller which generates joint torque commands with consideration of whole body dynamics and other constraints. In Section IV, simulations are performed on the humanoid robot WALK-MAN using the proposed control strategy. The paper ends up with conclusions and an outlook for future researches.

II. SIMPLIFIED MODEL AND ANALYSIS

For on-line planning, a simplified, especially linear model is preferred to provide a longer preview horizon. Nevertheless, it is difficult to consider complicated constraints, such as the kinematic constraint of legs. To realize straight leg walking, our idea is using LIMP for planning but considering the kinematic constraint in low-level controller which involves the whole body dynamic model of the robot. More detailedly, we will set the predefined height of LIPM a bit higher than the maximum reachable one. And then the low-level controller will try its best to stretch the leg to track the desired height but still meet the constraints. To evaluate its feasibility, ZMP derivation caused by the proposed control strategy is analyzed below.

In LIPM, the CoM moves in a constant height which results in bent-knee motions. Here, assume the legs of humanoid robots are fully extended and the resulted CoM motion follows a inverted pendulum swing curve. The induced vertical motion will lead to ZMP deviation from the one planned by LIPM.

(a) Model (b) Trajectory and ZMP deviation
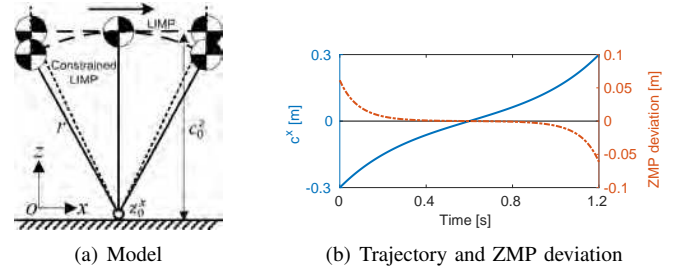
Fig. 2.   Simplified model and ZMP deviation in sagittal plane.

(a) Model (b) Trajectory and ZMP deviation
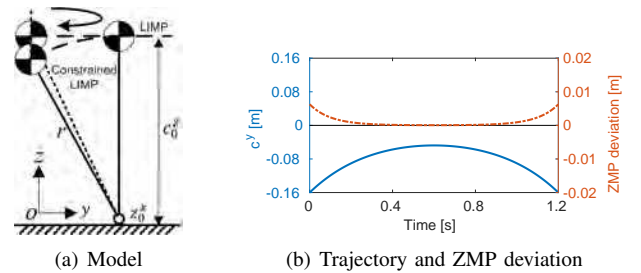
Fig. 3.   Simplified model and ZMP deviation in lateral plane.

Considering the motion of CoM of a robot, the ZMP constraints could be expressed as a nonlinear differential equation:

$$c^{\mathrm{x,y}} - \frac{mc^{\mathrm{z}}\ddot{c}^{\mathrm{x,y}} - \boldsymbol{S}\dot{\boldsymbol{L}}^{\mathrm{x,y}}}{m(\ddot{c}^{\mathrm{z}} + g^{\mathrm{z}})} = z^{\mathrm{x,y}} \in conv\{p_i\} \qquad (1)$$

where c stands for the motion of CoM and z for ZMP, m is the total mass of robot and $\boldsymbol{L}$ is the angular momentum around CoM. g is the gravitational acceleration constant. Those superscripts indicate the motion coordinate. $conv\{p_i\}$ represents the convex hull of contact points and $\boldsymbol{S}$ is a simple rotation matrix [17].

Since we mainly focus on straight knee strategy and will not manipulate angular momentum to help balancing, angular momentum is going to be neglected in the following analyses. In this case, the ZMP constraint is simplified to:

$$c^{\mathrm{x,y}} - \frac{c^{\mathrm{z}}}{\ddot{c}^{\mathrm{z}} + g^{\mathrm{z}}}\ddot{c}^{\mathrm{x,y}} = z^{\mathrm{x,y}} \in conv\{p_i\} \qquad (2)$$

Assuming the reference CoM trajectory is planned based on LIPM with constant desired CoM height c_0^{z} and desired ZMP at the center of foot $z^{\mathrm{x,y}} = 0$. The resulting CoM dynamic could be derived by substituting c_0^{z} and $\ddot{c}^{\mathrm{z}} = 0$ to equation (2):

$$\begin{cases} \ddot{c}^{\mathrm{x,y}} = g^{\mathrm{z}}\dfrac{c^{\mathrm{x,y}}}{c_0^{\mathrm{z}}} \\ \ddot{c}^{\mathrm{z}} = 0 \end{cases} \qquad (3)$$

The ordinary differential equations (3) have analytic solutions [18]:

$$c^{\mathrm{x,y}} = c^{\mathrm{x,y}}(0)\cosh(t/T_c) + T_c\dot{c}^{\mathrm{x,y}}(0)\sinh(t/T_c)$$
$$T_c = \sqrt{c_0^{\mathrm{z}}/g} \qquad (4)$$

Where t is the time, $c^{x,y}(0)$ and $\dot{c}^{x,y}(0)$ are the initial position and velocity of CoM. To further simplify the analysis, we consider the CoM motion in sagittal (x-z) and lateral (y-z) plane separately. As mentioned above, in order to make the robot walk with straight leg, the desired CoM height c_0^z will be set higher than the maximum reachable one r. And this would encourage the robot to stretch the legs as much as possible. In this case, the resulting CoM motion achieved by low-level controller will be an arc. So the CoM position and acceleration along z direction are:

$$c^z = \sqrt{r^2 - (c^{x,y})^2}$$
$$\ddot{c}^z = -\frac{c^{x,y}\ddot{c}^{x,y}}{c^z} - \frac{(\dot{c}^{x,y})^2}{c^z} - \frac{(c^{x,y}\dot{c}^{x,y})^2}{(c^z)^3} \quad (5)$$

It should be noted that actually r is not constant and will change when the robot is moving like lifting its swing leg. But here for simplicity, we assume it is constant. Substitute equations (5) into (2), we get the ZMP deviation caused by the CoM vertical variation:

$$z^{x,y} = c^{x,y} - \frac{(c^z)^4 \ddot{c}^{x,y}}{(g^z c^z - c^{x,y}\ddot{c}^{x,y} - (\dot{c}^{x,y})^2)(c^z)^2 - (c^{x,y}\dot{c}^{x,y})^2} \quad (6)$$

According to equation (4), (5), (6), the deviation of ZMP is related to the time t, initial position $c^{x,y}(0)$ and velocity $\dot{c}^{x,y}(0)$ of CoM, CoM's maximum reachable length r and the desired CoM height c_0^z. To ensure the knees stretching straight during walking, c_0^z should not be smaller than r. Here we set $c_0^z = r = 1$ m which is similar to the CoM height of WALK-MAN in its static standing posture. We can calculate the ZMP deviations in sagittal and lateral planes by setting typical initial states. The initial position and velocity for the sagittal plane are -0.3 m and 0.98 m/s while the ones for lateral plane are -0.16 m and 0.48 m/s when left leg is supporting alone. Fig. 2 and 3 show the ZMP deviations in the two directions. Blue solid line is the CoM trajectory and red dash-dot line is the ZMP deviation. The maximum ZMP derivation in lateral plane is less than 1 cm , quite small compared with foot width 16 cm while the one in sagittal plane is around 6 cm. However since the foot size is also longer (30 cm) in sagittal plane, the deviation is acceptable. This analysis result indicates it is possible to plan CoM trajectory via LIPM with an unreachable CoM height and then try to consider the constraints neglected by the simplified model in low level controller. More details about our control method are introduced below.

III. CONTROL FRAMEWORK

The control framework consists of a high-level part and a low-level part. The high-level controller generates gait patterns using Model Predictive Control scheme with LIPM as its internal model [19]. The low-level controller is formulated as a quadratic optimization problem to generate joint torques according to given tasks with respect to constraints, such as dynamic feasibility, friction cone, torque limits.

Walking is actually a multi-task motion. It involves cartesian space trajectory tracking, partial body posture regulation while maintaining dynamic balance. While dealing with multiple tasks, traditional null-space projection based techniques could be applied to solve the problem in a hierarchical manner [20] [21]. But this analytical techniques can not properly handle inequality constraints, such as torque limit and friction cone limit. Researchers turn to numerical method which is better at considering different constraints. Although detailed formulations differ, most of approaches formulate the floating base inverse dynamics as a quadratic programming (QP) problem with equality and inequality constraints [22]–[26].

Quadratic formulation is adopted to solve whole body dynamics. Different weights are used to balance multiple tasks in the cost function without considering strict priorities among them. It is simple to implement and also numerically robust. Hard constraints such as joint torque limits and friction cone limits are formulated as inequality constraints. We will give details about our low-level controller, starting from the Equation of Motion (EoM) of the whole robot:

$$\mathbf{M}(\mathbf{q})\ddot{\mathbf{q}} + \mathbf{h}(\mathbf{q},\dot{\mathbf{q}}) = \mathbf{S}^T\boldsymbol{\tau} + \mathbf{J}_c^T(\mathbf{q})\boldsymbol{\lambda} \quad (7)$$

with the inertia matrix $\mathbf{M}(\mathbf{q})$, the force vector $\mathbf{h}(\mathbf{q})$ which is sum of Coriolis, centrifugal and gravitational forces and the ground reaction force $\boldsymbol{\lambda}$. $\mathbf{J}_c^T$ is corresponding Jacobian, $\boldsymbol{\tau}$ is joint torque, $\mathbf{q}$ represents the n degrees of freedom (DoF) generalized coordinates which include base and body joint coordinate $\mathbf{q} = [\mathbf{q}_f^T, \mathbf{q}_r^T]^T$, and $\mathbf{S} = [\mathbf{0}_{n_r \times n_f}, \mathbf{I}_{n_r}]$ is a selection matrix which separates the $n_r = n - n_f$ actuated joints from the $n_f = 6$ floating-base DoFs.

EoM (7) relates generalized acceleration $\ddot{\mathbf{q}}$, contact forces $\boldsymbol{\lambda}$ and joint torques $\boldsymbol{\tau}$ together. We choose $\mathbf{X} = [\ddot{\mathbf{q}}^T, \boldsymbol{\lambda}^T]^T$ as optimization variables for the following QP problem :

$$\min_{\mathbf{X}} \sum_{i=1}^{n} \frac{\omega_i}{2} ||\mathbf{A_i}\mathbf{X} - \mathbf{b_i}||^2 \quad (8)$$

subject to

$$\mathbf{M_f}(\mathbf{q})\ddot{\mathbf{q}} + \mathbf{h_f}(\mathbf{q},\dot{\mathbf{q}}) = \mathbf{J}_{cf}^T(\mathbf{q})\boldsymbol{\lambda} \quad (9)$$

$$\boldsymbol{\tau} = \mathbf{S}(\mathbf{M}(\mathbf{q})\ddot{\mathbf{q}} + \mathbf{h}(\mathbf{q},\dot{\mathbf{q}}) - \mathbf{J}_c^T(\mathbf{q})\boldsymbol{\lambda}) \in [\boldsymbol{\tau}_{\min}, \boldsymbol{\tau}_{\max}] \quad (10)$$

$$\mathbf{J}_c\ddot{\mathbf{q}} + \dot{\mathbf{J}}_c\dot{\mathbf{q}} = \mathbf{0} \quad (11)$$

$$|\frac{f_x}{f_z}| \le \mu, \ |\frac{f_y}{f_z}| \le \mu \quad (12)$$

$$d_x^- \le \frac{m_y}{f_z} \le d_x^+, \ d_y^- \le -\frac{m_x}{f_z} \le d_y^+ \quad (13)$$

The objective function tries to minimize the tracking error of different tasks, but their relative importance is decided by corresponding weight ω_i. Tasks usually involve: motion tasks (regulating CoM position or tracking end-effectors' space trajectory), contact force tasks (optimizing contact force distribution) and joint torque tasks (assigning joint torques).

The constraints (9) and (10) ensure the dynamics feasibility and joint torque limits, the subscript f in (9) stands for the six DoFs of floating base. (11) makes sure there is no slip in contact points. The contact wrench can be expressed as: $\boldsymbol{\lambda} = [f_x, f_y, f_z, m_x, m_y, m_z]^{\mathrm{T}}$. The nonlinear friction cone is approximated as a linear polyhedral cone in which constraint (12) makes the contact force stay. (13) restricts ZMP stay inside support polygon which is defined within the limits $[d_x^-, d_x^+]$ and $[d_y^-, d_y^+]$.

Using this formulation, each task is defined by corresponding matrix $\mathbf{A}_{\text{task}}$ and $\mathbf{b}_{\text{task}}$.

1) Motion tasks: Motion task is one of most common tasks that robots are required to perform. Here, two examples are given: CoM trajectory tracking and end-effector trajectory tracking.

For CoM tracking, considering the centroidal dynamics [27], the system's linear momentum $\mathbf{P}$ and angular momentum $\mathbf{L}$ is linear with the generalized velocity $\dot{\mathbf{q}}$:

$$\begin{bmatrix} \mathbf{P} \\ \mathbf{L} \end{bmatrix} = \mathbf{H}(\mathbf{q})\dot{\mathbf{q}} \tag{14}$$

with $\mathbf{H}$ is called the centroidal momentum matrix. Taking derivative of this equation will give:

$$\begin{bmatrix} \dot{\mathbf{P}} \\ \dot{\mathbf{L}} \end{bmatrix} = \mathbf{H}\ddot{\mathbf{q}} + \dot{\mathbf{H}}\dot{\mathbf{q}} \tag{15}$$

It is obvious that the changing rate of momentum $\dot{\mathbf{P}}$ and $\dot{\mathbf{L}}$ is linear function of $\ddot{\mathbf{q}}$. As a result, the task matrix below could be used to track desired changing rate of momentum:

$$\mathbf{A}_{\text{H}} = [\mathbf{H}, \ \mathbf{0}], \ \mathbf{b}_{\text{H}} = \begin{bmatrix} \dot{\mathbf{P}}_{\text{ref}} \\ \dot{\mathbf{L}}_{\text{ref}} \end{bmatrix} - \dot{\mathbf{H}}\dot{\mathbf{q}} \tag{16}$$

Typically, reference changing rate of momentum could be defined as:

$$\begin{bmatrix} \dot{\mathbf{P}}_{\text{ref}} \\ \dot{\mathbf{L}}_{\text{ref}} \end{bmatrix} = \begin{bmatrix} \dot{\mathbf{P}}_{\text{des}} \\ \dot{\mathbf{L}}_{\text{des}} \end{bmatrix} + \mathbf{K}_{\text{p}} \begin{bmatrix} \mathbf{c}_{\text{des}} - \mathbf{c} \\ \mathbf{0} \end{bmatrix} + \mathbf{K}_{\text{d}} \begin{bmatrix} \mathbf{P}_{\text{des}} - \mathbf{P} \\ \mathbf{L}_{\text{des}} - \mathbf{L} \end{bmatrix} \tag{17}$$

with $\mathbf{K}_{\text{p}}$ and $\mathbf{K}_{\text{d}}$ the gains of the PD feedback controller.

Trajectory tracking for end-effector in Cartesian space is formulated as:

$$\mathbf{A}_{\text{cartesian}} = [\mathbf{J}, \ \mathbf{0}], \ \mathbf{b}_{\text{cartesian}} = \ddot{\mathbf{x}}_{\text{ref}} - \dot{\mathbf{J}}\dot{\mathbf{q}} \tag{18}$$

with $\mathbf{J}$ the spacial jacobian matrix corresponding to the frame attached to the robot. $\ddot{\mathbf{x}}_{\text{ref}}$ is the reference spacial acceleration which can be calculated with:

$$\ddot{\mathbf{x}}_{\text{ref}} = \ddot{\mathbf{x}}_{\text{des}} + \mathbf{K}_{\text{p}}(\mathbf{x}_{\text{des}} - \mathbf{x}) + \mathbf{K}_{\text{d}}(\dot{\mathbf{x}}_{\text{des}} - \dot{\mathbf{x}}) \tag{19}$$

where $\mathbf{x}_{\text{des}}$, $\dot{\mathbf{x}}_{\text{des}}$ and $\ddot{\mathbf{x}}_{\text{des}}$ are desired end-effectors' position, velocity and acceleration.

2) Contact force tasks: Sometimes it is required for the robot to control its contact force with the environment. This could be achieved by formulation:

$$\mathbf{A}_{\text{force}} = [\mathbf{0}, \ \mathbf{I}], \ \mathbf{b}_{\text{force}} = \boldsymbol{\lambda}_{\text{des}} \tag{20}$$

with $\boldsymbol{\lambda}_{\text{des}}$ the desired contact forces.

3) Joint torque tasks: To directly control joint torque, the task could be formulated as:

$$\mathbf{A}_{\tau} = \mathbf{S}[\mathbf{M}, \ \mathbf{J}_{\text{c}}^{\mathrm{T}}], \ \mathbf{b}_{\tau} = \boldsymbol{\tau}_{\text{des}} - \mathbf{S}\mathbf{h} \tag{21}$$

with $\boldsymbol{\tau}_{des}$ is the desired joint torque vector.

IV. SIMULATION

To evaluate the effectiveness and performance, the proposed control method was tested on WALK-MAN [28] in ROS-Gazebo simulation environment. WALK-MAN contains 31 DoFs with height around 1.9 m and total mass 130 Kg. It has two 6 DoFs legs and two 7 DoFs arms, and others are for waist and neck joints. Each joint is torque controlled with combined feed-forward and feedback terms:

$$\boldsymbol{\tau} = \boldsymbol{\tau}_{\text{ref}} + K_p(\mathbf{q}_{\text{ref}} - \mathbf{q}) + K_d(\dot{\mathbf{q}}_{\text{ref}} - \dot{\mathbf{q}}) + K_i \int (\mathbf{q}_{\text{ref}} - \mathbf{q}) \tag{22}$$

Where $\boldsymbol{\tau}_{\text{ref}}$ is the joint torque computed from inverse dynamics as (10), $\mathbf{q}_{\text{ref}}$ and $\dot{\mathbf{q}}_{\text{ref}}$ are the joint position and velocity integrated from the joint acceleration which is forepart of the optimization variable (8). K_p, K_d and K_i are PID gains for the feedback term. Here we didn't use the integration item and set $K_i = 0$. Feed-forward torque dominates the control command while feedback gains are so small that the robot can not even stand up without feed-forward torques. The control frequency is 500 Hz.

In this simulation, the high-level controller used LMPC to generate the CoM and foot trajectories first. Since the CoM height during straight standing is around 1.15 m, therefore we set the desired CoM height of LIPM to 1.17 m to let the low-level controller enforce leg straightening during walking. The z direction is vertical while x is along forward direction and y is lateral. The time of each step is 1.5 second, and no double-support phase is considered except the starting and ending steps. The foot placement is determined automatically by the high-level controller, but for the ending step, the foot placement is set the same with the starting step in y direction. Besides, the CoM terminal position of starting and ending steps and terminal velocity of each step is also assigned. The detailed trajectories generated by high-level controller can refer to Fig. 4.

The objectives set for this simulation in low-level controller were to track the CoM and foot trajectories, and keep upper body upright. At the same time, the low-level controller also ensured that the kinematic and dynamic constraints were satisfied. So even when the trajectories planned by high-level controller were not tracked very strictly, the ZMP constraints would still be satisfied by low-level controller. We set the desired CoM height a little higher than maximum and try to track it as well as possible via low-level controller. Fig. 1 shows the snapshots of WALK-MAN walking with straight legs and Fig. 4 presents the simulation data.

In Fig. 4, the blue solid line is the measured data collected from simulated WALK-MAN robot and the red dash-dot line is the desired one planned by high-level controller. The CoM

(a) CoM trajectory in x direction.

(b) CoM trajectory in y direction.

(c) CoM trajectory in z direction.

(d) ZMP trajectory in x direction.

(e) ZMP trajectory in y direction.
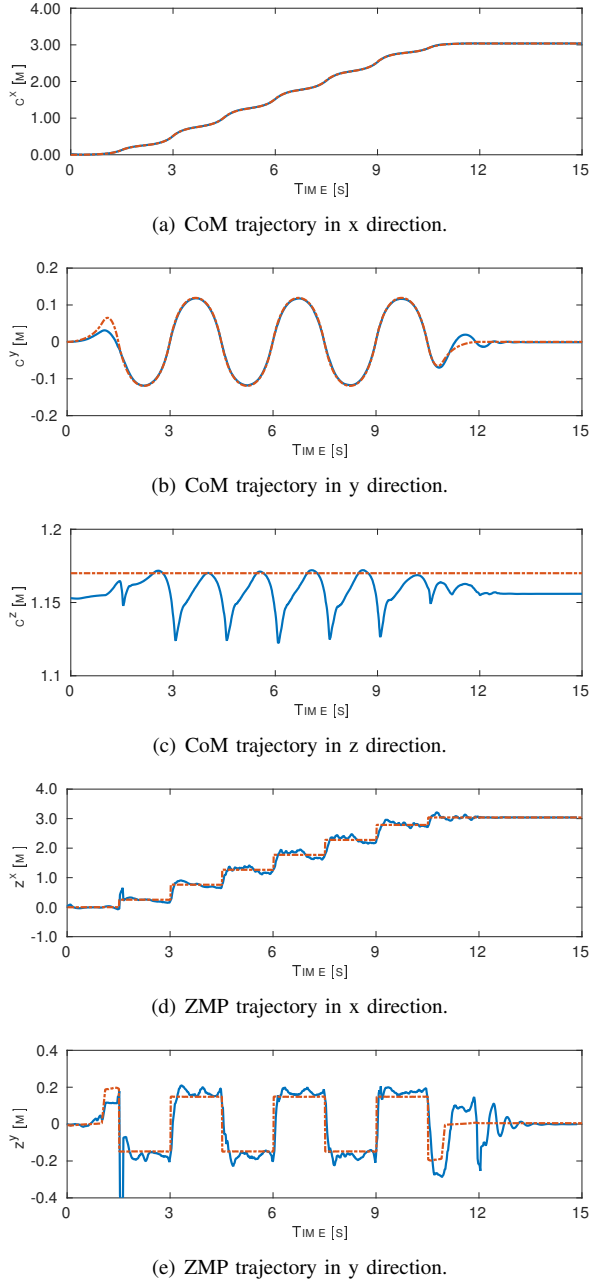
Fig. 4. CoM and ZMP trajectories when walking straight (blue solid line is measured and red dash-dot line is desired).

Fig. 5. CoM trajectory projected in front y-z plane.

(a) Knee trajectory.

(b) Knee torque.
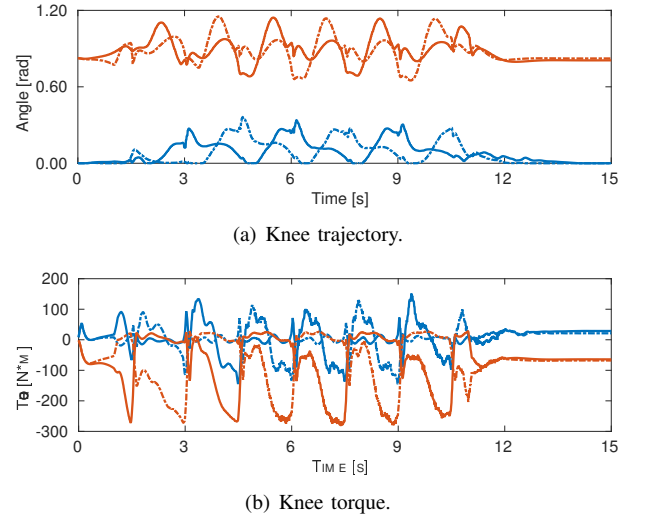
Fig. 6. Knee position and torque data (blue solid and dash-dot lines are for left and right straight legs, red solid and dash-dot lines are for left and right bent legs).

and ZMP trajectories along x direction were tracked quite well while the ones along y direction were a bit worse. It is because less ankle torque can be used to keep stable and maintain precise tracking in y direction due to smaller foot width compared with its length. Notable result in this simulation data is the CoM tracking along z direction. We can see it was not tracked strictly, instead, it oscillated under the desired height just as we expected. Besides, during walking CoM height was possible to be higher than the one when the robot was standing straight just as shown in Fig. 4(c), because the robot needed to lift its swing leg for walking and

the maximum CoM reachable height would increase. The CoM heights at the beginning and the end of walking were different, because the robot postures at the two moments were not exactly the same and corresponding maximum CoM reachable heights were different. Fig. 5 shows the CoM trajectory in the front y-z plane and it is quite similar with the typical butterfly shape observed in human walking [29].

To compare our proposed control strategy with the normal LIPM one with low CoM height, we let the robot walk in simulation again but with a constant CoM height 1.1 m. The robot can track the planned CoM trajectory very well but needs much bigger torque in knee joints. Fig. 6 shows the comparison result. Blue lines are collected from our control strategy while red ones are for the walking with constant CoM height 1.1 m which is typical for WALK-MAN robot generating LIPM walking pattern. And solid and dash-dot lines represent left and right knees separately. By using our control strategy, the knee angles are quite close to zero and the corresponding joint torques are almost half of the ones with constant low CoM height. High energy efficiency is promised for our control strategy. This simulation result supported our hypothesis well and proved the feasibility of our methods.

5

V. Conclusion

To reduce required torque in knee joints and improve energy efficiency, this paper proposed a new strategy to realize human-like straight leg walking. An optimal controller is designed and it consists of high-level part and low-level part. In the high-level controller, a reference CoM trajectory is generated based on LIPM using LMPC. Low-level controller uses quadratic programing to optimize joint torque commands which takes the whole body dynamics into account and can follow the reference CoM trajectory fairly well. To encourage straight leg walking, we set the desired CoM height of LIPM a little higher than the maximum reachable one. In this case, the motion in x and y direction of CoM is strictly tracked but the planned trajectory in z direction will be revised by the low level controller due to the kinematic limit of legs. The ZMP deviation caused by the revision is also studied and proved to be quite small. Besides the ZMP constraint is also properly handled through GRF distribution in the low-level controller, so this control strategy won't make the foot rotate. Simulation performed on WALK-MAN shows the CoM trajectory in the frontal plane forms a typical butterfly shape similar to human walking, and much less torque is needed in the knee joints compared with walking with low constant CoM height.

This study provides a different view to realize straight leg walking for humanoid robots. High energy efficiency and low torque requirement in knee joints are promised. In the future, we will implement it to the real robot and try to combine it with other manipulation tasks to make the robot more versatile.

References

[1] F. Massaad, T. M. Lejeune, and C. Detrembleur, "The up and down bobbing of human walking: a compromise between muscle work and efficiency," *The Journal of physiology*, vol. 582, no. 2, pp. 789–799, 2007.

[2] R. Alexander, "Mcn.(1992) exploring biomechanics. animals in motion," *Scientific American Library, New York*, vol. 247.

[3] T. McGeer, "Passive dynamic walking," *the international journal of robotics research*, vol. 9, no. 2, pp. 62–82, 1990.

[4] S. Kajita, F. Kanehiro, K. Kaneko, K. Yokoi, and H. Hirukawa, "The 3d linear inverted pendulum mode: A simple modeling for a biped walking pattern generation," in *International Conference on Intelligent Robots and Systems*, vol. 1, 2001, pp. 239–246.

[5] J. Pratt, J. Carff, S. Drakunov, and A. Goswami, "Capture point: A step toward humanoid push recovery," in *International Conference on Humanoid Robots*, 2006, pp. 200–207.

[6] F. Iida, Y. Minekawa, J. Rummel, and A. Seyfarth, "Toward a human-like biped robot with compliant legs," *Robotics and Autonomous Systems*, vol. 57, no. 2, pp. 139–144, 2009.

[7] M. Morisawa, S. Kajita, K. Kaneko, K. Harada, F. Kanehiro, K. Fujiwara, and H. Hirukawa, "Pattern generation of biped walking constrained on parametric surface," in *International Conference on Robotics and Automation*, 2005, pp. 2405–2410.

[8] K. Terada and Y. Kuniyoshi, "Online gait planning with dynamical 3d-symmetrization method," in *International Conference on Humanoid Robots*, 2007, pp. 222–227.

[9] Z. Li, N. G. Tsagarikis, D. G. Caldwell, and B. Vanderborght, "Trajectory generation of straightened knee walking for humanoid robot icub," in *International Conference on Control Automation Robotics and Vision*, 2010, pp. 2355–2360.

[10] J. Englsberger, C. Ott, and A. Albu-Schäffer, "Three-dimensional bipedal walking control based on divergent component of motion," *Transactions on Robotics*, vol. 31, no. 2, pp. 355–368, 2015.

[11] Y. Ogura, K. Shimomura, H. Kondo, A. Morishima, T. Okubo, S. Momoki, H.-o. Lim, and A. Takanishi, "Human-like walking with knee stretched, heel-contact and toe-off motion by a humanoid robot," in *International Conference on Intelligent Robots and Systems*, 2006, pp. 3976–3981.

[12] M. H. Raibert *et al.*, *Legged robots that balance*. MIT press Cambridge, MA, 1986, vol. 3.

[13] Y. YOU, Z. LI, N. G. TSAGARAKIS, and D. G. CALDWELL, "Foot placement control for bipedal walking on uneven terrain: An online linear regression analysis approach," in *International Conference on Climbing and Walking Robots and Support Technologies for Mobile Machines*, 2015, p. 478.

[14] K. Van Heerden, "Planning com trajectory with variable height and foot position with reactive stepping for humanoid robots," in *International Conference on Robotics and Automation*, 2015, pp. 6275–6280.

[15] S. Feng, X. Xinjilefu, W. Huang, and C. G. Atkeson, "3d walking based on online optimization," in *International Conference on Humanoid Robots*, 2013, pp. 21–27.

[16] C. Brasseur, A. Sherikov, C. Collette, D. Dimitrov, and P.-B. Wieber, "A robust linear mpc approach to online generation of 3d biped walking motion," in *International Conference on Humanoid Robots*, 2015, pp. 595–601.

[17] P.-B. Wieber, R. Tedrake, and S. Kuindersma, "Modeling and control of legged robots," in *Springer Handbook of Robotics*. Springer, 2016, pp. 1203–1234.

[18] S. Kajita, H. Hirukawa, K. Harada, and K. Yokoi, *Introduction to humanoid robotics*. Springer, 2014, vol. 101.

[19] A. Herdt, N. Perrin, and P.-B. Wieber, "Walking without thinking about it," in *International Conference on Intelligent Robots and Systems*, 2010, pp. 190–195.

[20] L. Sentis and O. Khatib, "A whole-body control framework for humanoids operating in human environments," in *International Conference on Robotics and Automation*, 2006, pp. 2641–2648.

[21] L. Sentis, "Synthesis and control of whole-body behaviors in humanoid systems," Ph.D. dissertation, Citeseer, 2007.

[22] M. de Lasa, I. Mordatch, and A. Hertzmann, "Feature-based locomotion controllers," in *ACM Transactions on Graphics (TOG)*, vol. 29, no. 4. ACM, 2010, p. 131.

[23] A. Escande, N. Mansard, and P.-B. Wieber, "Hierarchical quadratic programming: Fast online humanoid-robot motion generation," *The International Journal of Robotics Research*, p. 0278364914521306, 2014.

[24] A. Herzog, L. Righetti, F. Grimminger, P. Pastor, and S. Schaal, "Balancing experiments on a torque-controlled humanoid with hierarchical inverse dynamics," in *International Conference on Intelligent Robots and Systems*, 2014, pp. 981–988.

[25] M. Hutter, H. Sommer, C. Gehring, M. Hoepflinger, M. Bloesch, and R. Siegwart, "Quadrupedal locomotion using hierarchical operational space control," *The International Journal of Robotics Research*, p. 0278364913519834, 2014.

[26] P. M. Wensing and D. E. Orin, "Generation of dynamic humanoid behaviors through task-space control with conic optimization," in *International Conference on Robotics and Automation*, May 2013, pp. 3103–3109.

[27] D. E. Orin, A. Goswami, and S.-H. Lee, "Centroidal dynamics of a humanoid robot," *Autonomous Robots*, vol. 35, no. 2-3, pp. 161–176, 2013.

[28] N. Tsagarakis, D. Caldwell, A. Bicchi, F. Negrello, M. Garabini, W. Choi, L. Baccelliere, V. Loc, J. Noorden, M. Catalano *et al.*, "Walk-man: A high performance humanoid platform for realistic environments," *Journal of Field Robotics (JFR)*, 2016.

[29] M. S. Orendurff, A. D. Segal, G. K. Klute, J. S. Berge *et al.*, "The effect of walking speed on center of mass displacement," *Journal of rehabilitation research and development*, vol. 41, no. 6A, p. 829, 2004.